

Estimating global agricultural effects of geoengineering using volcanic eruptions

Jonathan Proctor^{1,2,7}*, Solomon Hsiang^{1,3,7}, Jennifer Burney⁴, Marshall Burke^{3,5} & Wolfram Schlenker^{3,6}

Solar radiation management is increasingly considered to be an option for managing global temperatures 1,2, yet the economic effects of ameliorating climatic changes by scattering sunlight back to space remain largely unknown³. Although solar radiation management may increase crop yields by reducing heat stress⁴, the effects of concomitant changes in available sunlight have never been empirically estimated. Here we use the volcanic eruptions that inspired modern solar radiation management proposals as natural experiments to provide the first estimates, to our knowledge, of how the stratospheric sulfate aerosols created by the eruptions of El Chichón and Mount Pinatubo altered the quantity and quality of global sunlight, and how these changes in sunlight affected global crop yields. We find that the sunlight-mediated effect of stratospheric sulfate aerosols on yields is negative for both C4 (maize) and C3 (soy, rice and wheat) crops. Applying our yield model to a solar radiation management scenario based on stratospheric sulfate aerosols, we find that projected mid-twentyfirst century damages due to scattering sunlight caused by solar radiation management are roughly equal in magnitude to benefits from cooling. This suggests that solar radiation managementif deployed using stratospheric sulfate aerosols similar to those emitted by the volcanic eruptions it seeks to mimic—would, on net, attenuate little of the global agricultural damage from climate change. Our approach could be extended to study the effects of solar radiation management on other global systems, such as human health or ecosystem function.

Geoengineering—the purposeful alteration of the climate to offset changes induced by greenhouse gas emissions—is a proposed, but still poorly understood, approach to limit future warming⁵. One of the most widely suggested geoengineering strategies is solar radiation management (SRM). SRM proposals typically involve spraying precursors to sulfate aerosols into the stratosphere to produce particles that cool the earth by reflecting sunlight back into space⁶. The closest natural analogues to these SRM proposals are major volcanic eruptions⁷. Eruptions of El Chichón (1982, Mexico) and Mount Pinatubo (1991, the Philippines) injected 7 and 20 Mt of sulfur dioxide, respectively, into the atmosphere, which was then oxidized to form stratospheric sulfate aerosols (SSAs)⁸. These particles propagated throughout the tropics over several weeks and spread latitudinally over the following months, increasing the opacity of the stratosphere—as measured by optical depth—more than an order of magnitude above baseline levels for multiple years (Fig. 1a-c, e).

The eruptions of El Chichón and Pinatubo had substantial effects on the global optical environment and climate. We analyse daily data from 859 insolation stations (n = 3,311,553) station-days; Fig. 1d) paired with stratospheric aerosol optical depth $(SAOD)^{10}$ and cloud fraction data under all-sky conditions. We find that the Pinatubo eruption (global average of +0.15 SAOD) reduced direct sunlight by 21%, increased diffuse sunlight by 20% and reduced total sunlight by 2.5% (Fig. 1f, Extended Data Table 1, Supplementary Information, section II).

These global all-sky results generalize previous clear-sky estimates at individual stations¹¹. Globally, this reduction in insolation led to cooling of about $0.5\,^{\circ}\mathrm{C^8}$ and redistribution and net reduction in precipitation¹², effects that were partially offset by a concurrent El Niño event (Fig. 2). On the basis of these observations, it has previously been suggested that SRM cooling could mitigate agricultural damages from global warming⁴. The net effect of SRM, however, remains uncertain owing to possible unintended consequences from SSA-induced changes. Here we empirically estimate how the alteration of sunlight by SSAs may directly affect agricultural yields, after accounting for effects mediated by temperature, precipitation and clouds.

The sign of the 'insolation effect' of SRM on agriculture is theoretically ambiguous^{13–16}. Scattering light decreases total available sunlight—which tends to decrease photosynthesis—but increases the fraction of light that is diffuse, which can increase photosynthesis by redistributing light from sun-saturated canopy leaves to shaded leaves below^{15,17}. It is unknown whether damages from decreasing total light or benefits from increasing diffuse light dominate in crop production. The sign of this insolation effect will depend primarily on two factors: the forward-scattering properties of the aerosol and the relative benefit of diffuse light for the growth of edible yield (Supplementary Information, section III.5). The latter may depend on canopy geometry, photosynthetic pathway (for example, C3 or C4) and ambient conditions 13,18. Previous studies of unmanaged ecosystems have tended to find that scattering increases biomass growth 15,19—although not always 18—and, importantly, that edible yield production may not directly correlate with biomass growth. Studies of agricultural systems tend to estimate the negative effects of tropospheric aerosol scattering^{13,16} and positive effects of solar brightening²⁰ on yields. Simulations of potential SRM effects focus on cooling and precipitation effects²¹ and suggest global yields may increase owing to cooling⁴, although these analyses do not account for the full effect of scattering. To our knowledge, this is the first study to estimate and account for the net effects of SSA radiative scattering on yields, thereby testing whether the benefits of SSA scattering demonstrated in unmanaged ecosystems^{15,19} also apply to agricultural production, as has often been hypothesized^{4,14}. This analysis is also, to our knowledge, the first global empirical study of the insolation effect on crops as well as the first study to leverage a quasi-experimental design to estimate the total effect of SRM on any economic sector.

The theoretically ideal experiment would measure the total effect of SRM on yields using many identical Earths, half of them treated with SSAs. In practice, we approximate this experiment with one Earth during sequential periods of high and low SSA exposure, exogeneously determined by volcanic eruptions. We identify the insolation effect of SSAs on yields²² (Extended Data Fig. 1) by comparing countries to themselves over time, with changing SSA treatment—measured in SAOD composited from satellite and other observations¹⁰ (Fig. 1e)—while controlling flexibly for potentially confounding climate variables, including temperature, precipitation, cloud fraction and the El

¹Global Policy Laboratory, Goldman School of Public Policy, University of California, Berkeley, Berkeley, CA, USA. ²Department of Agricultural and Resource Economics, University of California, Berkeley, Berkeley, CA, USA. ³National Bureau of Economic Research, Cambridge, MA, USA. ⁴School of Global Policy and Strategy, University of California, San Diego, San Diego, CA, USA. ⁵Department of Earth System Science, Stanford University, Stanford, CA, USA. ⁶School of International and Public Affairs and The Earth Institute, Columbia University, New York, NY, USA. ⁷These authors contributed equally: Jonathan Proctor, Solomon Hsiang. *e-mail: proctor@berkeley.edu

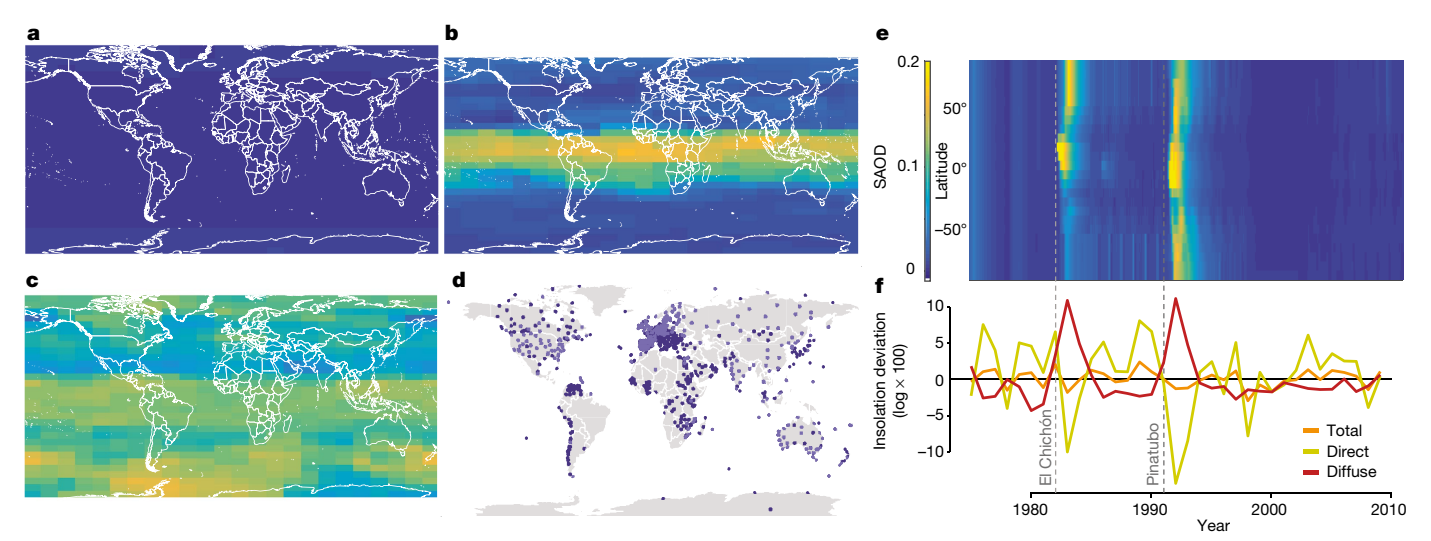


Fig. 1 | Large volcanic eruptions alter the global optical environment. \mathbf{a} – \mathbf{c} , SAOD (1,000 nm) before the Pinatubo eruption (March 1991) (\mathbf{a}), two months after the eruption (August 1991) (\mathbf{b}) and the next year, after the aerosol cloud had spread (March 1992) (\mathbf{c}). \mathbf{d} , Surface insolation observing stations used in our analysis of the effect of SAOD on insolation; light blue stations additionally measure diffuse light. \mathbf{e} , SAOD (550 nm)

from 1975–2010¹⁰. **f**, Annual average daily total (orange), direct (yellow) and diffuse (red) sunlight across all stations; before averaging, each measurement at a given station on a given day-of-year was de-meaned (by subtracting the mean of all observations from the respective station and day-of-year), to remove seasonal effects as well as differences in geography and observational protocols.

Niño–Southern Oscillation (ENSO) (Supplementary Information, section III.3). Our multivariate fixed-effects panel estimation strategy (equation (16) in Supplementary Information) accounts for unobserved time-invariant factors—such as soil type or historical propensity for civil unrest—as well as country-specific time-trending variables, such as access to fertilizers or trends in damaging tropospheric ozone²³. Our primary analysis focuses on the Pinatubo eruption because the concentration and distribution of resulting SSAs were measured with substantially more accuracy than were those of earlier eruptions²⁴. We validate the model by verifying that the estimated responses of crop yields to temperature and precipitation are consistent with previous studies²⁵ (Extended Data Fig. 2).

We find that the changes in sunlight from SSAs reduce both C4 (maize; P < 0.01, n = 2,501 country-years) and C3 (soy, rice and wheat; P < 0.05, n = 4,828 crop-country-years) yields, by 48% and 28%, respectively, per unit SAOD (Fig. 3a, model 1). This indicates that the global average scattering from Pinatubo (+0.15 SAOD) reduced C4 yields by 9.3% and C3 yields by 4.8% (Fig. 3b), although some of this loss was probably offset by SSA-induced cooling, making it difficult to observe directly. By contrast, process models and empirical analyses of unmanaged-ecosystem biomass growth tend to estimate a positive insolation effect, which suggests that either the diffuse fertilization effect is weaker for crops than ecosystems or scattering light alters the relative production of biomass and edible yield.

Our finding that SSA scattering from Pinatubo negatively affected yields is robust to removing temperature, precipitation, ENSO and cloud controls (Fig. 3a, models 2–5), estimating the effect separately for each crop, accounting for the zenith angle of incoming sunlight, using two alternative datasets of SSA SAOD, dropping observations from the countries in which the major eruptions occurred and adding surface $\rm CO_2$ as a control (Extended Data Table 2). We examine the effect of future, current and past SSAs on current yields, finding that only contemporaneous exposure to SSAs matters (Fig. 3d). We estimate the yield–insolation response flexibly, and fail to reject that the response is linear over the support of our data (Extended Data Fig. 3).

Extending the analysis back in time increases the sample size but also the measurement error, owing to weaknesses in the historical observational system. The estimated insolation effect for both C3 and C4 crops becomes smaller, and remains significant for C4 crops, as we sequentially include data from the eruptions of El Chichón (1982) (Fig. 3a, model 6) and Agung (1963) (Extended Data Table 2 column 9). This

pattern is consistent with both systematic 'attenuation bias' from the mis-measurement of SAOD before the satellite era²⁶ and differences in the radiative properties of the SSAs generated by Pinatubo and El Chichón, discussed below.

Two results support the idea that our analysis captures a sunlight-mediated effect. First, the response of C3 crops is less negative than that of C4 crops (P < 0.01). C3 crops benefit from scattering more than

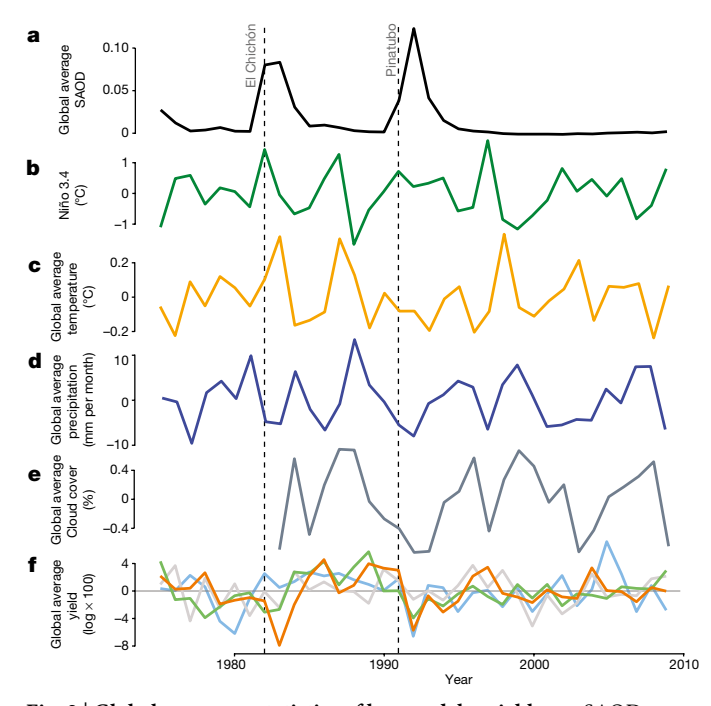


Fig. 2 | Global summary statistics of key model variables. a, SAOD for years after the eruptions of El Chichón (March to April 1982) and Pinatubo (June 1991) (dotted lines). b—e, The ENSO 3.4 index (b), surface air temperature (c), precipitation (d) and cloud fraction (e) during the same period. f, Yields of maize (orange), wheat (grey), soy (blue) and rice (green) decline after the eruptions. Climate and yield values are growing-season averages, de-trended by country-specific quadratic time trends and averaged over countries in the sample. SAOD data are processed similarly, but are not de-trended.

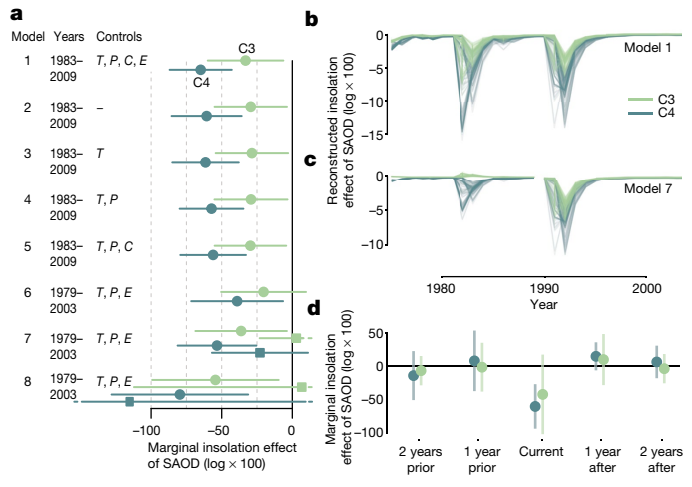


Fig. 3 | Empirical estimates of the insolation effect of SSAs on crop yield. a, The estimated effect of increasing SSA optical depth by one unit on C4 (blue) and C3 (green) yields, owing to changes in sunlight (model 1, equation (16) in Supplementary Information, and Extended Data Table 2). Models 2−5 drop and then sequentially add temperature (*T*), precipitation (*P*), cloud (*C*) and ENSO (*E*) controls. Models 7−8 estimate effects separately for Pinatubo (year ≥ 1990, circles) and Chichón (year < 1990, squares); Model 8 uses a different SAOD dataset (SPARC). b, Reconstructions of the SSA insolation effect using model 1. Each line represents a single country over time. c, As in b, but using model 7. d, Simultaneously estimated insolation effects two years before and two years after the current growing season. See Supplementary Information sections III.2.3, III.2.2 and III.4. In a, d, whiskers represent 95% confidence intervals.

C4 crops because the C3 photosynthetic rate saturates at lower light levels¹³. Second, per unit of SAOD, aerosols from El Chichón are both more forward scattering (Extended Data Tables 1, 3) and less damaging to yields (Fig. 3a, models 7, 8) than those of Pinatubo. This pattern is consistent with diffuse fertilization increasing edible yield. It also suggests that aerosol radiative properties may explain some heterogeneity in the estimated insolation effect across these eruptions. This heterogeneity substantially affects reconstructed yield losses from SSA scattering (Fig. 3c). We are, however, unable to determine whether this difference in the estimated insolation effect across eruptions is due to a difference in the radiative properties of the SSAs or to a differing degree of measurement error and, in turn, attenuation bias (Supplementary Information, section III.6).

To calculate the total effect of SSAs on yields for a future SRM scenario, we apply our empirical results (Fig. 3a, model 1) to output

from an earth system model and compare future yields under two scenarios: (1) climate change under Representative Concentration Pathway 4.5 (RCP4.5)—a modest mitigation pathway—and (2) the same, but with sulfur dioxide injection to balance all additional anthropogenic forcing after 2020²⁷.

Over cropped areas in this simulation (2050–2069), the SRM treatment (average \pm 0.084 SAOD) decreases the average temperature by 0.88 °C, reduces precipitation by 0.26 mm per month and increases the cloud fraction by 0.0081 relative to the control during the maize growing season (Extended Data Fig. 4). In turn, average maize yields increase by 6.3% owing to this cooling (Fig. 4a), decrease by 5.3% owing to SRM-induced dimming (Fig. 4b) and change by <0.2% owing to altered precipitation and clouds (Fig. 4c, d). We sum these partial effects to construct the total effect of SRM, and repeat the analysis for soy, rice and wheat (Extended Data Fig. 5). We find that, relative to the control, SRM treatment has no statistically discernible effect on yields once we have accounted for optical effects (P > 0.1 for all crops; Fig. 4e, Extended Data Fig. 6). Failing to account for the insolation effect, as was done in the only previous global estimate⁴, substantially overestimates the benefits of SRM to agriculture.

Our analysis finds that volcanogenic SSAs have statistically significant and economically substantial insolation-mediated costs that are roughly equal in magnitude to their benefits from cooling. This suggests that anthropogenic SSAs used in SRM may not be able to substantially lessen the risks that climate change poses to global agricultural yields and food security (Extended Data Fig. 7).

Our finding that SSAs from El Chichón were more forward scattering and less damaging than SSAs from Pinatubo indicates that optimizing the radiative properties of particles used in SRM might mitigate insolation-mediated damages. However, we cannot rule out the possibility that this difference was due instead to poor observation of the SSAs from El Chichón.

Farmer-level adaptations, such as switching to varieties more resistant to dimming, could theoretically mitigate the insolation-mediated damage of SRM. However, given that farmer-level adaptations to extreme heat have been modest²⁸, it is not clear that adaptation to dimming will be easier.

Our quasi-experimental results are consistent with the sunlight-mediated effect of tropospheric aerosols ¹⁶ and emissions of their precursors ²⁹ on Indian wheat and rice yields, further supporting the notion that we capture a sunlight-mediated response. It is however possible that other factors, such as increased ultraviolet-light exposure from stratospheric ozone destruction, could explain part of the estimated effect. Notably, changes in tropospheric ozone concentrations due to Pinatubo are thought to be negative ³⁰, which would increase yields—suggesting that our results might underestimate the SSA insolation effect.

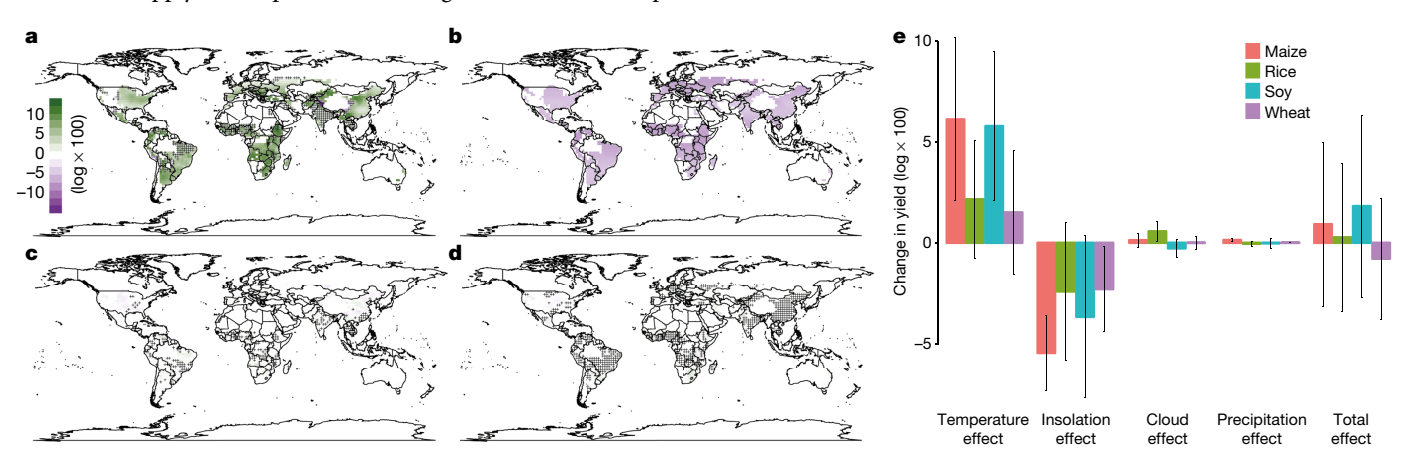


Fig. 4 | Partial and total effects of SRM on yields. a–d, The partial effects of SRM—relative to a climate-change-only scenario (RCP4.5)—on expected maize yields from 2050–2069, owing to changes in temperature (a), insolation (b), precipitation (c) and cloud fraction (d). Statistically insignificant changes (P > 0.05) are hatched. Changes in uncropped land

have been masked out by setting the values to zero. e, Global partial and total effects of SRM (cropped-fraction weighted average) for maize (red), soy (turquoise), rice (green) and wheat (purple). Error bars show 95% confidence intervals for the predicted effect.



Online content

Any Methods, including any statements of data availability and Nature Research reporting summaries, along with any additional references and Source Data files, are available in the online version of the paper at https://doi.org/10.1038/s41586-018-0417-3.

Received: 18 June 2017; Accepted: 29 June 2018; Published online 8 August 2018.

- Crutzen, P. J. Albedo enhancement by stratospheric sulfur injections: a contribution to resolve a policy dilemma? Clim. Change 77, 211–219 (2006).
- Ocean Studies Board. Climate Intervention: Reflecting Sunlight to Cool the Earth (The National Academies, Washington DC, 2015).
- MacMartin, D. G., Kravitz, B., Long, J. C. S. & Rasch, P. J. Geoengineering with stratospheric aerosols: what do we not know after a decade of research? *Earths Future* 4, 543–548 (2016).
- Pongratz, J., Lobell, D. B., Cao, L. & Caldeira, K. Crop yields in a geoengineered climate. Nat. Clim. Change 2, 101–105 (2012).
- Pachauri, R. K. et al. Climate Change 2014: Synthesis Report. Contribution of Working Groups I, II and III to the Fifth Assessment Report of the Intergovernmental Panel on Climate Change (eds Core Writing Team, Pachauri, R. K. & Meyer, L. A.) (IPCC, Geneva, 2015).
- Robock, A., Marquardt, A., Kravitz, B. & Stenchikov, G. Benefits, risks, and costs of stratospheric geoengineering. *Geophys. Res. Lett.* 36, L19703 (2009).
- Robock, A., MacMartin, D. G., Duren, R. & Christensen, M. W. Studying geoengineering with natural and anthropogenic analogs. *Clim. Change* 121, 445–458 (2013).
- 8. Robock, A. Volcanic eruptions and climate. Rev. Geophys. 38, 191–219 (2000).
- World Radiation Data Centre. 'Global radiation. Daily sums, monthly sums and means' and 'Diffuse radiation. Daily sums, monthly sums and means'. World Meteorological Organization http://wrdc.mgo.rssi.ru/ (accessed 1 August 2015).
- Sato, M., Hansen, J. E., McCormick, M. P. & Pollack, J. B. Stratopheric aerosol optical depths 1850–1990. J. Geophys. Res. 98, 22987–22994 (1993).
- Dutton, E. G. & Christy, J. R. Solar radiative forcing at selected locations and evidence for global lower tropospheric cooling following the eruptions of El Chichón and Pinatubo. *Geophys. Res. Lett.* 19, 2313–2316 (1992).
- Trenberth, K. E. & Dai, A. Effects of Mount Pinatubo volcanic eruption on the hydrological cycle as an analog of geoengineering. *Geophys. Res. Lett.* 34, L15702 (2007).
- 13. Greenwald, R. et al. The influence of aerosols on crop production: a study using the CERES crop model. *Agric. Syst.* **89**, 390–413 (2006).
- Roderick, M. L. & Farquhar, G. D. Geoengineering: hazy, cool and well fed? Nat. Clim. Change 2, 76–77 (2012).
- Gu, L. et al. Response of a deciduous forest to the Mount Pinatubo eruption: enhanced photosynthesis. Science 299, 2035–2038 (2003).
- Gupta, R., Somanathan, E. & Dey, S. Global warming and local air pollution have reduced wheat yields in India. Clim. Change 140, 593–604 (2017).
- Roderick, M. L., Farquhar, G. D., Berry, S. L. & Noble, I. R. On the direct effect of clouds and atmospheric particles on the productivity and structure of vegetation. *Oecologia* 129, 21–30 (2001).
- Alton, P. B. Reduced carbon sequestration in terrestrial ecosystems under overcast skies compared to clear skies. Agric. For. Meteorol. 148, 1641–1653 (2008)
- Mercado, L. M. et al. Impact of changes in diffuse radiation on the global land carbon sink. *Nature* 458, 1014–1017 (2009).

- Tollenaar, M., Fridgen, J., Tyagi, P., Stackhouse, P. W. Jr. & Kumudini, S. The contribution of solar brightening to the US maize yield trend. *Nat. Clim. Change* 7, 275–278 (2017).
- Xia, L. et al. Solar radiation management impacts on agriculture in China: a case study in the Geoengineering Model Intercomparison Project (GeoMIP). J. Geophys. Res. Atmos. 119, 8695–8711 (2014).
- Food and Agriculture Organization of the United Nations. Crops, NationalProduction. FAOSTAT http://www.fao.org/faostat/en/#data/QC (accessed 1 January 2016).
- 23. Hsiang, S. Climate econometrics. Annu. Rev. Resour. Econ. 8, 43-75 (2016).
- Thomason, L. & Peter, T. (eds) SPARC Assessment of Stratospheric Aerosol Properties (ASAP). SPARC Report No. 4 http://www.sparc-climate.org/ publications/sparc-reports/ (SPARC Scientific Streering Group, 2006).
- Schlenker, W. & Lobell, D. B. Robust negative impacts of climate change on African agriculture. *Environ. Res. Lett.* 5, 014010 (2010).
- Wooldridge, J. M. Econometric Analysis of Cross Section and Panel Data (MIT Press, Cambridge, 2002).
- Niemeier, U., Schmidt, H., Alterskjær, K. & Kristjánsson, J. E. Solar irradiance reduction via climate engineering: impact of different techniques on the energy balance and the hydrological cycle. *J. Geophys. Res. Atmos.* 118, 11905–11917 (2013).
- Carleton, T. A. & Hsiang, S. M. Social and economic impacts of climate. Science 353, aad9837 (2016).
- Burney, J. & Ramanathan, V. Recent climate and air pollution impacts on Indian agriculture. Proc. Natl Acad. Sci. USA 111, 16319–16324 (2014).
- Tang, Q., Hess, P. G., Brown-Steiner, B. & Kinnison, D. E. Tropospheric ozone decrease due to the Mount Pinatubo eruption: reduced stratospheric influx. *Geophys. Res. Lett.* 40, 5553–5558 (2013).

Acknowledgements We thank M. Anderson, M. Auffhammer, D. Baldocchi, K. Caldeira, C. Field, A. Goldstein, D. Keith, P. Huybers, R. Kopp, D. Lobell, K. Ricke, J. Sallee and seminar participants at Berkeley, Chicago, Columbia, Cornell, Harvard, Johns Hopkins and Stanford universities, the Massachusetts Institute of Technology and the Allied Social Science Association Annual Meeting for useful comments. We thank I. Bolliger for his contributions to the project and all the members of the Global Policy Laboratory for their valuable feedback. We thank L. Thomason for generously sharing SAOD data used in Fig. 1a–c. This material is based upon work supported by the National Science Foundation Grant No. CNH-L 1715557 and the National Science Foundation Graduate Research Fellowship under Grant No. DGE 1752814.

Reviewer information *Nature* thanks L. Gu and the other anonymous reviewer(s) for their contribution to the peer review of this work.

Author contributions S.H. conceived the study; J.P., S.H., J.B., M.B. and W.S. designed the study; J.P. collected and analysed the data with contributions from J.B.; J.P., S.H., J.B., M.B. and W.S. interpreted results; J.P. and S.H. wrote the paper.

Competing interests The authors declare no competing interests.

Additional information

Extended data is available for this paper at https://doi.org/10.1038/s41586-018-0417-3.

Supplementary information is available for this paper at https://doi.org/10.1038/s41586-018-0417-3.

Reprints and permissions information is available at http://www.nature.com/reprints.

Correspondence and requests for materials should be addressed to J.P. **Publisher's note:** Springer Nature remains neutral with regard to jurisdictional claims in published maps and institutional affiliations.



METHODS

No statistical methods were used to predetermine sample size.

To link national annual yield data from the Food and Agricultural Organization of the United Nations to climatological data, we aggregate all gridded temperature, precipitation, cloud and SAOD datasets to the annual-country level by averaging values over cropped area 31 to the growing season 32 using a methodology that is similar to those previously published 25,33 .

Our analysis of the effect of SSAs on log insolation (n = 3,311,553 station-days for total insolation and 889,327 for direct and diffuse insolation) models SAOD, cloud fraction³⁴ and ENSO (current and lagged) linearly (equation (2) in Supplementary Information). We include station by day-of-year fixed effects. Our analysis of the effect of SSAs on atmospheric forward scattering shares the same specification (equation (5) in Supplementary Information).

Our analysis of the effect of SSAs on log yields models the effect of SAOD linearly (nonlinear estimates do not significantly differ from the linear estimate; Extended Data Fig. 3), the response of temperature³⁵, precipitation³⁶ and clouds³⁷ using restricted cubic splines, and allows the response of ENSO (current and lagged) to differ between teleconnected and non-teleconnected regions³⁸ (equation (16) in Supplementary Information). We include country fixed effects and country-specific quadratic time trends. For all empirical insolation and yield analyses we calculate standard errors to account for serial correlation within countries across years and for spatial autocorrelation within years across countries²³.

To calculate the total effect of SRM relative to a climate change scenario, we average results over three ensemble members from the Max Planck Institute Earth System Model²⁷. Uncertainty in the total effect represents uncertainty in the estimated parameters of the empirical yield model (Supplementary Information, section IV.4). We do not consider carbon fertilization effects in calculation

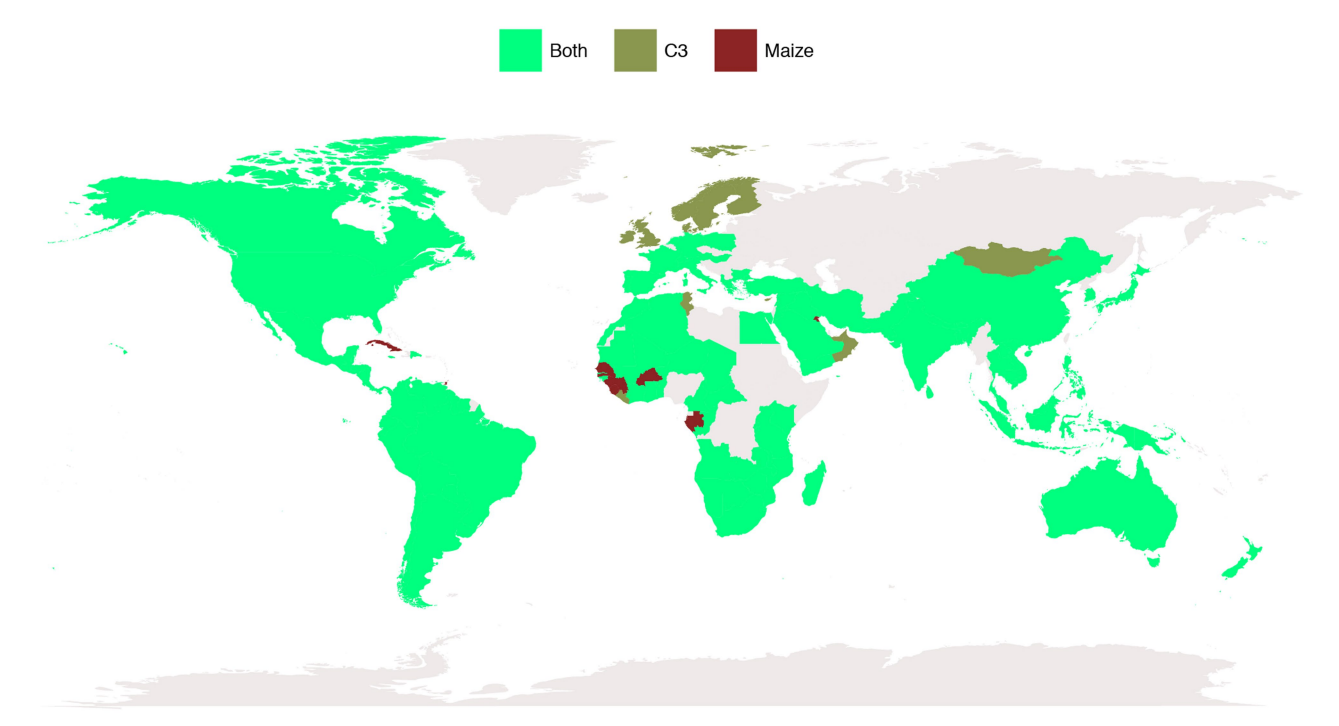
of the total effect because carbon dioxide levels are the same in the SRM and climate-change-only scenarios.

Reporting summary. Further information on experimental design is available in the Nature Research Reporting Summary linked to this paper.

Code availability. Replication code is available at https://zenodo.org/communities/global-agricultural-effects-of-geoengineering-volcanic-eruptions/ as well as upon request from the corresponding author.

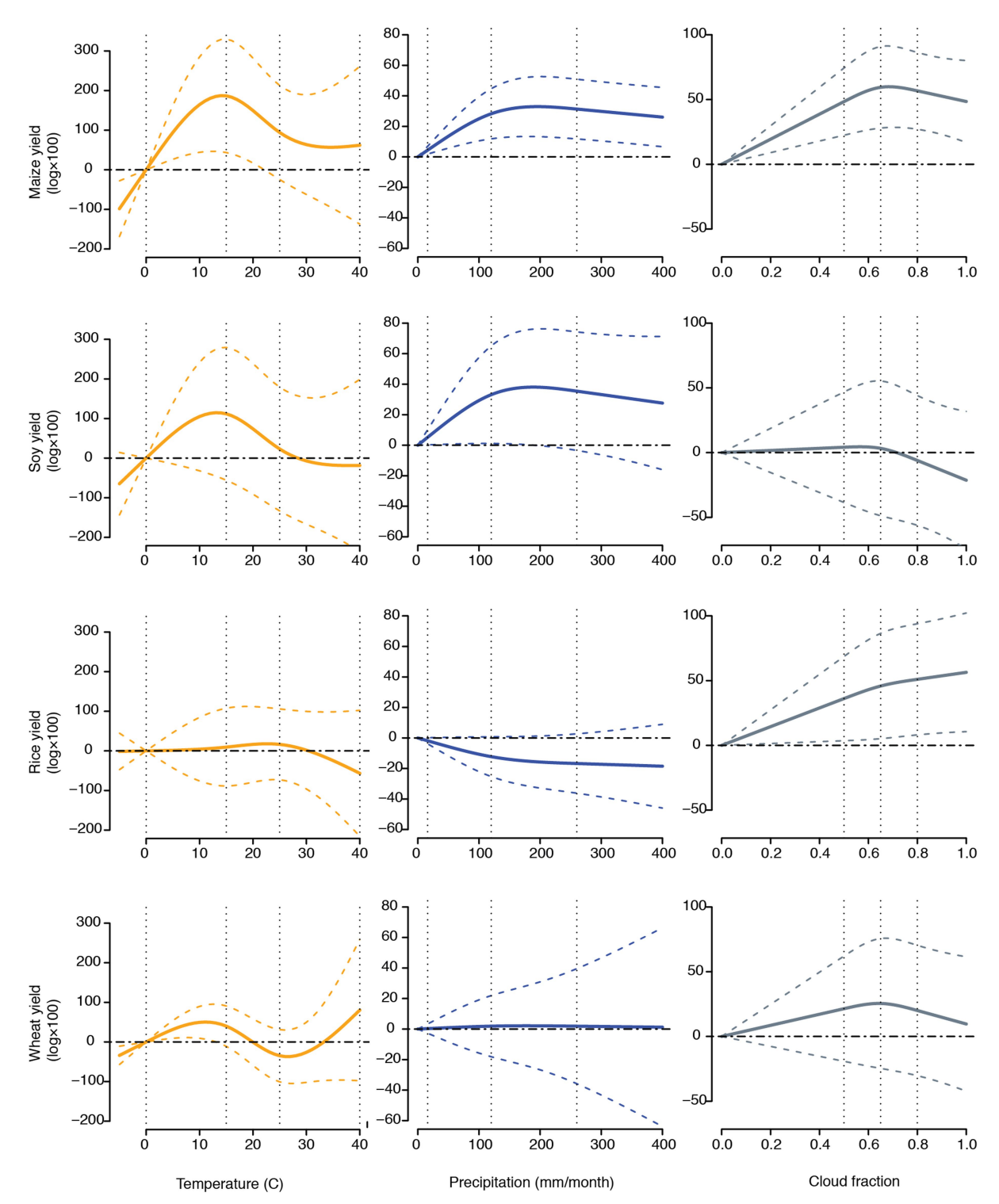
Data availability. All data used in this analysis is from free, publicly available sources and is available upon request from the corresponding author.

- Ramankutty, N., Evan, A. T., Monfreda, C. & Foley, J. A. Farming the planet: 1. geographic distribution of global agricultural lands in the year 2000. *Glob. Biogeochem. Cycles* 22, GB1003 (2008).
- Sacks, W. J., Deryng, D., Foley, J. A. & Ramankutty, N. Crop planting dates: an analysis of global patterns. *Glob. Ecol. Biogeogr.* 19, 607–620 (2010).
- Burke, M. & Emerick, K. Adaptation to climate change: evidence from US agriculture. Am. Econ. J. Econ. Policy 8, 106–140 (2016).
- ISCCP Science Team. ISCCP data and information. NASA Atmospheric Science Data Center https://eosweb.larc.nasa.gov/project/isccp/isccp_table (accessed 7 February 2016) (1999).
- 35. Rohde, R. et al. A new estimate of the average Earth surface land temperature spanning 1753 to 2011. *Geoinfor. Geostat. Overview* **1**, 1000101 (2013).
- Willmott, C. & Matsurra, K. Terrestrial air temperature and precipitation: monthly and annual time series (1950–1999). Earth System Research Laboratory http://www.esrl.noaa.gov/psd/ (accessed 1 January 2016) (2001).
- Norris, J. R. & Evan, A. T. Empirical removal of artifacts from the ISCCP and PATMOS-x satellite cloud records. *J. Atmos. Ocean. Technol.* 32, 691–702 (2015)
- Hsiang, S. M. & Meng, K. C. Tropical economics. Am. Econ. Rev. 105, 257–261 (2015).



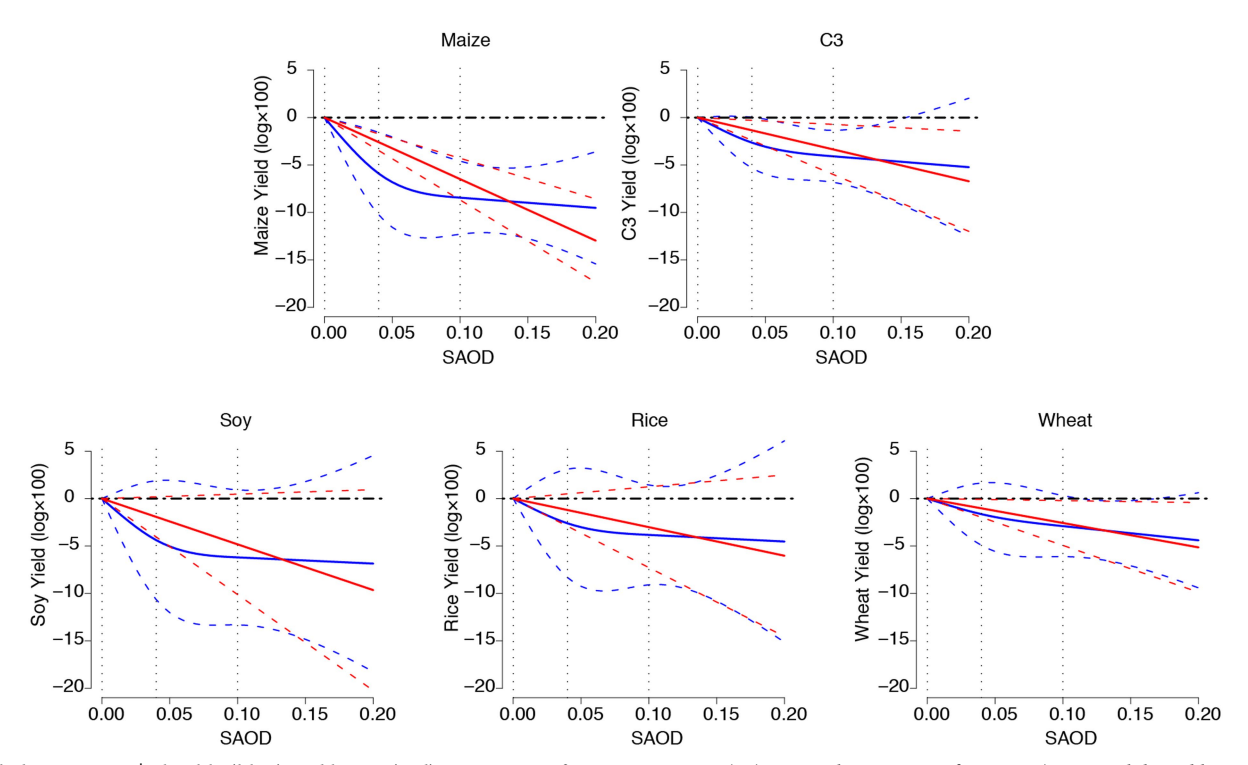
Extended Data Fig. 1 | Countries included in the estimation of the insolation-mediated effect of SAOD on crop yield. Countries in light green are included in the estimation of the insolation-mediated effect of SSAs on yields for both C3 (soy, rice and wheat) and C4 (maize) crops.

Countries in dark green are included only in estimation of the insolation effect for C3 crops, and countries in red are included only in estimation of the insolation effect for maize. Countries in grey are not included in the analysis owing to missing data.



Extended Data Fig. 2 | Estimated response of yields to changes in growing-season average temperature (orange), precipitation (blue) and cloud fraction (grey). Temperature, precipitation and cloud fraction axes show growing-season means. The y axes show partial effects on yield relative to a value of zero for each climatological variable ($f_{\rm T}(T_{it})$, $f_{\rm P}(P_{it})$

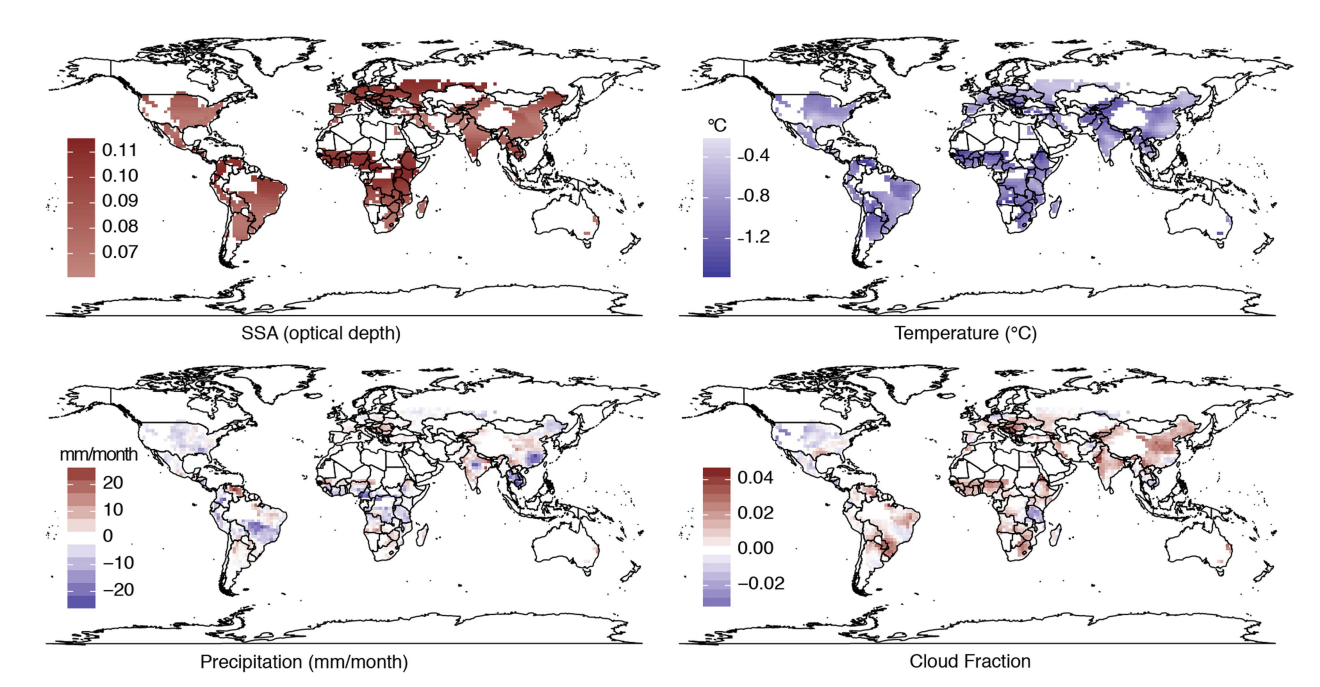
and $f_C(C_{it})$ in equation (16) in Supplementary Information). Vertical dotted lines show the placement of the knots for the restricted cubic splines specification. Dashed lines show the 95% confidence intervals. n = 2,501, 1,256, 1,562 and 2,010 country-years for maize, soy, rice and wheat, respectively.



Extended Data Fig. 3 | Flexible (blue) and linear (red) estimation of the insolation-mediated effect of SSAs on crop yields. The SAOD axes show growing-season means. Each point on a curve gives the optical effect of SAOD, relative to a value of zero (the slope of the red lines is β in

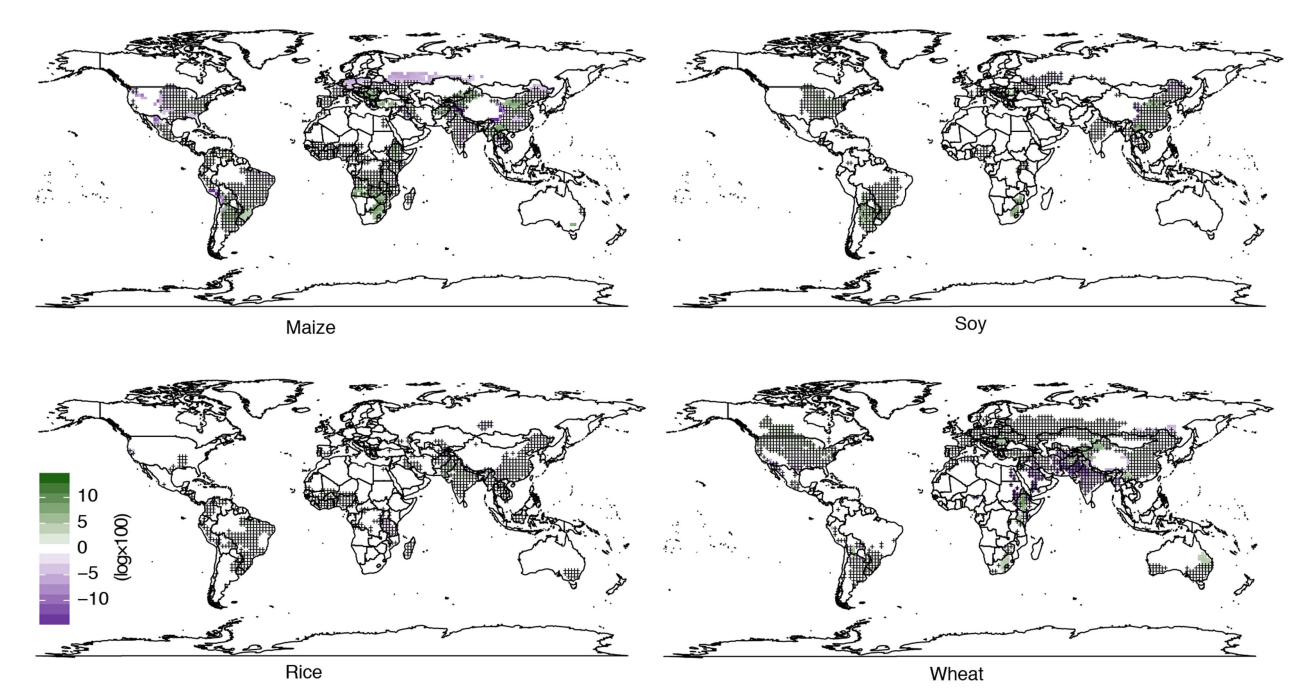
equation (16) in Supplementary Information). Vertical dotted lines show the placement of the knots for the restricted cubic splines specification. Dashed lines show the 95% confidence intervals.





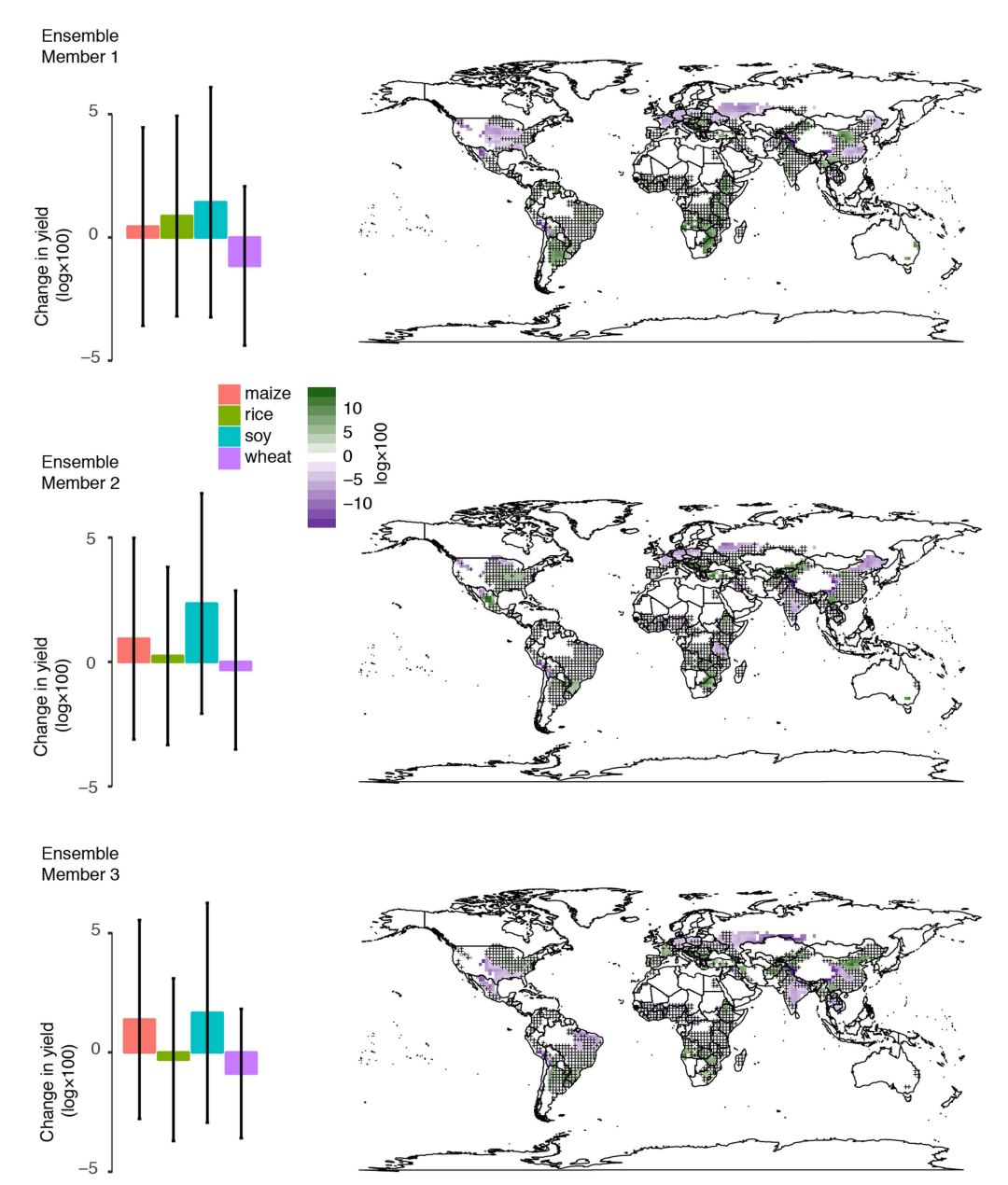
Extended Data Fig. 4 | Effect of SRM on climatological determinants of yield. SRM-induced changes in maize growing-season average SAOD, temperature, precipitation and cloud fraction, relative to the

climate-change-only scenario. Changes in uncropped land have been masked out by setting the values to zero.



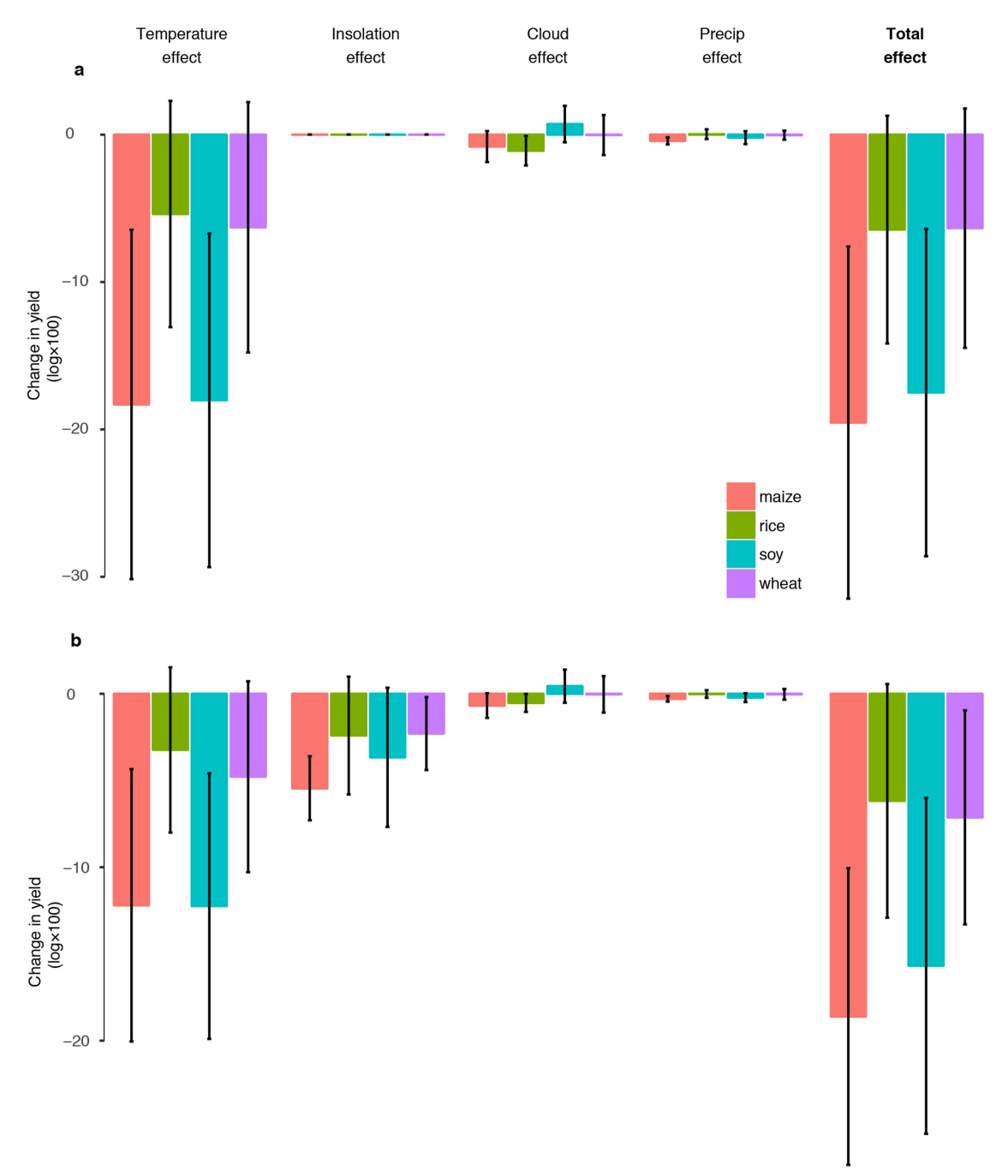
Extended Data Fig. 5 | Total effect of SRM on maize, soy, rice and wheat yields. Total effects are constructed by summing the partial effects from insolation, temperature, precipitation and clouds. Effects are relative to the climate-change-only scenario. Changes in uncropped land have been masked out by setting the values to zero. Statistically insignificant effects (P > 0.05) are hatched. We calculate P values using a two-sided

t-test comparing the estimated effect of SRM to a null hypothesis of zero effect. When calculating the distribution of the estimated SRM effect, we consider only statistical uncertainty. This uncertainty is shown in Extended Data Table 2, Extended Data Fig. 2, and the calculations are described in Supplementary Information, section IV.4.



Extended Data Fig. 6 | The finding that SRM mitigates little of the damages of climate change is consistent across three ensemble runs. Bar graphs show the total effect of SRM on global yields (cropped-fraction weighted average), relative to the climate change control, for each of the three Earth system model runs. Results are similar across ensemble member runs. Maps on the right show the total effect of SSAs on maize yields for each of the ensemble runs. Error bars in the bar graphs show 95% confidence intervals for estimated mean effects for each crop.

Statistically insignificant effects (P > 0.05) are hatched in the maps. Changes in uncropped land have been masked out by setting the values to zero. We calculate P values using a two-sided t-test comparing the estimated effects to a null hypothesis of zero effect. Within each ensemble member, we calculate the distributions of the estimated effects considering only statistical uncertainty. This uncertainty is shown in Extended Data Table 2, Extended Data Fig. 2, and the calculations are described in Supplementary Information, section IV.4.



Extended Data Fig. 7 | Effects of climate change and SRM relative to an historical scenario. a, As in Fig. 4e, but comparing a climate change scenario (RCP 4.5) to an historical scenario (Supplementary Information, section IV.3). b, As in Fig. 4e, but comparing a climate-change-with-SRM scenario to an historical scenario. Note that these calculations consider

only climatological and sunlight-mediated effects; changes in yields owing to carbon fertilization, or other factors that may differ between scenarios, are not included. Error bars show 95% confidence intervals around the estimated mean effect.



Extended Data Table 1 | Effect of SSAs on total, direct and diffuse insolation

Radiation Type: Years in Sample:	(1) Total [83-09]	(2) Total [79-09]	(3) Total [79-09]	(4) Direct [83-09]	(5) Direct [79-09]	(6) Direct [79-09]	(7) Diffuse [83-09]	(8) Diffuse [79-09]	(9) Diffuse [79-09]
SAOD	-0.172*** (0.062)	-0.067 (0.058)		-1.580*** (0.320)	-1.395*** (0.295)		1.199*** (0.122)	1.197*** (0.125)	
SAOD × (yr≤89) [Chichón]			-0.024 (0.079)			-1.039 (0.760)			2.063*** (0.102)
SAOD × (yr>89) [Pinatubo]			-0.100* (0.054)			-1.406*** (0.301)			1.171*** (0.115)
Cloud Fraction	-0.946*** (0.041)			-2.792*** (0.179)			0.499*** (0.085)		
Nino 3.4	0.002 (0.002)	0.002 (0.003)	0.002 (0.003)	0.018** (0.009)	0.017 (0.012)	0.017 (0.012)	-0.001 (0.003)	0.0004 (0.003)	0.001 (0.003)
Nino 3.4 (lagged)	0.004 (0.003)	-0.001 (0.003)	-0.001 (0.003)	0.006 (0.010)	-0.011 (0.013)	-0.011 (0.013)	-0.003*** (0.001)	0.001 (0.001)	0.0003 (0.002)
Observations Adjusted R ²	3,311,553 0.766	4,371,586 0.750	4,371,586 0.750	889,327 0.552	1,000,776 0.413	1,000,776 0.413	889,327 0.722	1,000,776 0.744	1,000,776 0.744

Coefficients on SAOD describe the effect of increasing SSA optical depth by 1 unit on the log of total, direct or diffuse sunlight. Columns 1, 4 and 7 show the preferred specification (equation (2) in Supplementary Information). Columns 2, 5 and 8 include data from 1979–2009 to capture the effect of both the Pinatubo and El Chichón eruptions. Columns 3, 6 and 9 estimate the effect separately for El Chichón and Pinatubo (Supplementary Information, section II.1). We do not control for cloud fraction in columns 2, 3, 5, 6, 8 and 9 because the cloud data are available only beginning in 1983. All models account for station-by-day-of-year fixed effects. Standard errors of the mean, shown in parentheses, are clustered by country and by year to account for serial correlation over time within a country and for autocorrelation across space within a year. We calculate P values using a two-sided t-test. *P < 0.1, **P < 0.05, ***P < 0.01.



Extended Data Table 2 | Robustness of the insolation effect of SSAs on yields to changes in model specification, data sample and data source

Name		(1)	(0)	(2)	(4)	(F)	(6)	(7)	(0)	(0)	(10)	(11)	(10)	(10)
Cox Cox Cox SPARC SP	Years in Sample	(1) [83-09]	(2) [83-09]	(3) [83-09]	(4) [83-09]	(5) [83-09]	(6) [83-09]	(7) [83-03]	(8) [83-05]	(9) [61-09]	(10) [83-09]	(11) [83-09]	(12) [79-03]	(13) [79-03]
Maine (C4) Mai	Climate Controls	None	Т	TP	TPC	TPCE	TPCE	TPCE	TPCE	TPE	TPCE	TPCEO	TPE	TPE
AOD	SAOD Data						Cos(SZA)	SPARC	SPARC2			Add CO ₂		SPARC
AAOD x (yr 89) (0.127) (0.120) (0.115) (0.118) (0.112) (0.0656) (0.252) (0.162) (0.125) (0.116) (0.119) (0.129) (0.173							Maize (C4)						
Pinatubo	SAOD × (yr≤89) [Chichón]												(0.173)	-1.073 (0.764) -0.796**
C3 - pooled C3 - poole C3 -	[Pinatubo] Observations												2,322	
SAOD	R-squared	0.950	0.952	0.953	0.953	0.954	0.954	0.953	0.955	0.939	0.953	0.954	0.948	0.949
Color Colo							<u>C3 - po</u>	oled						
Observations 4,828 4,828 4,828 4,828 4,828 4,828 4,828 3,618 3,916 7,431 4,694 4828 4,480 4,297 0,942 0,943 0,946 0,946 0,948 0,941 0,941 0,942 0,942 0,943 0,946 0,946 0,928 0,941 0,942 0,942 0,943 0,943 0,943 0,943 0,943 0,943 0,944 0,943 0,942 0,943 0,944 0,943 0,944 0,943 0,944 0,943 0,944 0,943 0,944 0,943 0,944 0,943 0,944 0,943 0,944 0,945 0,945 0,944 0,944 0,944 0,945	SAOD × (yr≤89) [Chichón] SAOD × (yr>89)												(0.132) -0.362**	0.0669 (0.606) -0.545**
SAOD	Observations												4,480	4,297
(0.287) (0.282) (0.276) (0.288) (0.270) (0.160) (0.381) (0.268) (0.270) (0.271) SAOD × (yr≤89) Chichdn SAOD × (yr≤89)							Soy (C	3)						
Chiechon	SAOD × (yr≤89) [Chichón] SAOD × (yr>89)												(0.236) -0.630**	(1.290) -0.843*
SAOD $(0.395^* - 0.407^* - 0.424^{**} - 0.412^* - 0.301 - 0.158 - 0.298 - 0.203 - 0.191 - 0.321 - 0.283 (0.295) (0.196) (0.198) (0.201) (0.202) (0.217) (0.118) (0.372) (0.267) (0.143) (0.228) (0.228) (0.225) (0.249) (0.245) (0.24$	Observations												1,169	1,118
$ \begin{array}{c ccccccccccccccccccccccccccccccccccc$							Rice (C	23)						
Pinatubo Chickon	SAOD × (yr≤89) [Chichón]												(0.244)	(1.059)
SAOD -0.201 -0.164 -0.161 -0.164 -0.257** -0.126** -0.594** -0.352* 0.103 -0.253**256** (0.127) (0.122) (0.122) (0.118) (0.121) (0.0600) (0.249) (0.200) (0.114) (0.123) (0.114) (0.123) (0.114) (0.156) (0.564) (0.166) (0	[Pinatubo] Observations R-squared												(0.251) 1,448	(0.368) 1,396
$ \begin{array}{c ccccccccccccccccccccccccccccccccccc$							Wheat ((C3)						
(Pinatubo) (0.158) (0.232) Observations 2,010 2,010 2,010 2,010 2,010 1,502 1,612 3,060 1,983 2,010 1,863 1,783	SAOD × (yr≤89) [Chichón]												(0.156)	0.0118 (0.564) -0.529**
	[Pinatubo] Observations R-squared												1,863	1,783

The table above shows the insolation effect of SSAs for maize, C3 crops pooled, and soy, rice and wheat yields individually across a range of robustness checks (Supplementary Information, section III.4). The C3 response is estimated assuming that crops that share the C3 photosynthetic pathway (soy, rice and wheat) have a common insolation effect (equation (18) in Supplementary Information). Columns 1–5 drop all climate controls and then add temperature (7), precipitation (*P*), cloud fraction (C) and ENSO (*E*) controls back in one at a time; column 5 is our preferred specification (equation (16) in Supplementary Information); column 6 accounts for the angle at which incoming light passes through the SSA layer by dividing SAOD by the cosine of the solar zenith angle (SZA); columns 7 and 8 use two alternative SSA datasets, SPARC and SPARC2 (Supplementary Information, section I.4); column 9 includes data from 1961–2009 to span the eruption of Agung; column 10 drops Mexico and the Philippines, where the EI Chichôn and Pinatubo eruptions occurred, from the analysis; column 11 adds surface CO₂ concentration as a control; column 12 estimates the effects for EI Chichôn and Pinatubo separately; and column 13 does the same using the SPARC dataset. All models account for country fixed effects and country-specific quadratic time trends. Standard errors of the mean, shown in parentheses, are clustered by country and by year to account for serial correlation over time within a country and for autocorrelation across space within a year. We calculate *P* values using a two-sided *t*-test. **P* < 0.1, ***P* < 0.05, **** *P* < 0.01.



Extended Data Table 3 | Effect of SSAs on atmospheric forward scattering

	(1)	(2)	(3)
Dep. Var. $= Pr(p$	hoton reaches	the surface	photon hits a particle)
Year	[83-09]	[79-09]	[79-09]
SAOD	0.233*** (0.030)	0.243*** (0.030)	
SAOD × (yr≤89) [Chichón]			0.345*** (0.031)
SAOD × (yr>89) [Pinatubo]			0.240*** (0.029)
Cloud Fraction	-0.047*** (0.018)		
Nino 3.4	0.001 (0.001)	0.001 (0.001)	0.001 (0.001)
Nino 3.4 (lagged)	-0.0004 (0.001)	-0.001 (0.001)	-0.001 (0.001)
Observations Adjusted R ²	886,287 0.228	997,142 0.227	997,142 0.227

The dependent variable is the probability that a photon of light makes it to the surface, conditional on hitting a particle (w in equation (3) in Supplementary Information). Coefficients on SAOD represent the effect of increasing SAOD by 1 unit on w for the entire atmospheric column. Column 1 is our preferred specification (equation (5) in Supplementary Information). Column 2 drops cloud controls and includes both the Pinatubo and El Chichón eruptions. Column 3 estimates the effects for El Chichón and Pinatubo separately. All models account for station-by-day-of-year fixed effects. Standard errors of the mean, shown in parentheses, are clustered by country and by year to account for serial correlation over time within a country and for autocorrelation across space within a year. We calculate P values using a two-sided t-test. ***P< 0.01.



|--|

Reporting Summary

Nature Research wishes to improve the reproducibility of the work that we publish. This form provides structure for consistency and transparency in reporting. For further information on Nature Research policies, see <u>Authors & Referees</u> and the <u>Editorial Policy Checklist</u>.

Statistical parameters

When statistical analyses are reported	, confirm that the following items are	e present in the relevant	location (e.g. fig	gure legend, ta	ble legend, mai
text, or Methods section).					

n/a	Со	nfirmed
	\boxtimes	The $\underline{\text{exact sample size}}$ (n) for each experimental group/condition, given as a discrete number and unit of measurement
\boxtimes		An indication of whether measurements were taken from distinct samples or whether the same sample was measured repeatedly
		The statistical test(s) used AND whether they are one- or two-sided Only common tests should be described solely by name; describe more complex techniques in the Methods section.
	$ \boxtimes$	A description of all covariates tested
	\boxtimes	A description of any assumptions or corrections, such as tests of normality and adjustment for multiple comparisons
		A full description of the statistics including <u>central tendency</u> (e.g. means) or other basic estimates (e.g. regression coefficient) AND <u>variation</u> (e.g. standard deviation) or associated <u>estimates of uncertainty</u> (e.g. confidence intervals)
		For null hypothesis testing, the test statistic (e.g. <i>F</i> , <i>t</i> , <i>r</i>) with confidence intervals, effect sizes, degrees of freedom and <i>P</i> value noted <i>Give P values as exact values whenever suitable.</i>
\boxtimes		For Bayesian analysis, information on the choice of priors and Markov chain Monte Carlo settings
\boxtimes		For hierarchical and complex designs, identification of the appropriate level for tests and full reporting of outcomes
\boxtimes		Estimates of effect sizes (e.g. Cohen's d , Pearson's r), indicating how they were calculated
		Clearly defined error bars State explicitly what error bars represent (e.g. SD, SE, CI)

Our web collection on statistics for biologists may be useful.

Software and code

Policy information about availability of computer code

Data collection

Stata 14, R version 3.4.3, Matlab 2017

Data analysis

Stata 14, R version 3.4.3, Matlab 2017

For manuscripts utilizing custom algorithms or software that are central to the research but not yet described in published literature, software must be made available to editors/reviewers upon request. We strongly encourage code deposition in a community repository (e.g. GitHub). See the Nature Research guidelines for submitting code & software for further information.

Data

Policy information about availability of data

All manuscripts must include a <u>data availability statement</u>. This statement should provide the following information, where applicable:

- Accession codes, unique identifiers, or web links for publicly available datasets
- A list of figures that have associated raw data
- A description of any restrictions on data availability

All data used in this analysis is from free, publicly available sources and is available upon request from the corresponding author.

							· C						•		
ΗI	el	C	l-S	Ŋ	е	CI	ΙŤΙ	C	re	D	0	rt	Ш	N	g
				1-						_					C J

Tread about the report this						
Please select the b	est fit for your research. If you are not sure, read the appropriate sections before making your selection.					
∑ Life sciences	Behavioural & social sciences Ecological, evolutionary & environmental sciences					
For a reference copy of	the document with all sections, see nature.com/authors/policies/ReportingSummary-flat.pdf					
Life scier	nces study design					
All studies must dis	sclose on these points even when the disclosure is negative.					
Sample size	For our primary analysis we used all national yield observations from the Food and Agricultural Organization of the United Nations Statistics Division from 1983-2009 for maize, soy, rice and wheat. We document all data management decisions in Supplementary Information Section 1. In our main yield analysis, N = 2,501, 1,256, 1,562, 2,010 for maize, soy, rice and wheat yields, respectively. In our main insolation analysis, N = 3,311,553, 889,327, and 889,327 for total, direct and diffuse light, respectively.					
Data exclusions	We included only countries that have no missing observations from 1983-2009 to balance the panel; notably, this drops countries created or dismantled by the break up of the Soviet Union in 1991. We document all data management decisions in Supplementary Information Section 1.					
Replication	The quasi-experimental research design does not allow us to explicitly reproduce the natural experiment; however, we subjected our results to all the standard checks and found it to be robust. These tests are detailed in Supplementary Information Section 3.4.					
Randomization	This was not an experiment; however, the paper's quasi-experimental design approximates an experiment by comparing countries to themselves over time with plausibly randomly assigned exposure to stratospheric volcanic aerosols. We detail the quasi-experimental research design in Supplementary Information Sections 3.1-3.3.					
Blinding	Blinding was not possible in this setting. Given the paper's historical quasi-experimental design and given that crops were the main subject, the traditional concerns with blinding (e.g. bias introduced by knowledge of one's treatment group) is not an issue. Blinding the analyst of the data was not possible given the need for extensive data cleaning and validation.					

Reporting for specific materials, systems and methods

Mat	terials & experimental systems	Methods			
n/a	Involved in the study	n/a	Involved in the study		
\boxtimes	Unique biological materials	\boxtimes	ChIP-seq		
\boxtimes	Antibodies	\times	Flow cytometry		
\boxtimes	Eukaryotic cell lines	\boxtimes	MRI-based neuroimaging		
\boxtimes	Palaeontology		•		
\boxtimes	Animals and other organisms				
\boxtimes	Human research participants				